8-1-2008

# Genome-wide transposon tagging reveals location-dependent effects on transcription and chromatin organization in Arabidopsis

Faye M. Rosin
*Rutgers University–New Brunswick*

Naohide Watanabe
*Rutgers University–New Brunswick*

Jean Luc Cacas
*Rutgers University–New Brunswick*

Naohiro Kato
*Rutgers University–New Brunswick*

Juana M. Arroyo
*Cold Spring Harbor Laboratory*

*See next page for additional authors*



## Recommended Citation

Rosin, F., Watanabe, N., Cacas, J., Kato, N., Arroyo, J., Fang, Y., May, B., Vaughn, M., Simorowski, J., Ramu, U., McCombie, R., Spector, D., Martienssen, R., & Lam, E. (2008). Genome-wide transposon tagging reveals location-dependent effects on transcription and chromatin organization in Arabidopsis. *Plant Journal, 55* (3), 514-525. https://doi.org/10.1111/j.1365-313X.2008.03517.x

the plant journal

SEB SOCIETY FOR EXPERIMENTAL BIOLOGY

*The Plant Journal* (2008) **55**, 514–525 doi: 10.1111/j.1365-313X.2008.03517.x

TECHNICAL ADVANCE

# Genome-wide transposon tagging reveals location-dependent effects on transcription and chromatin organization in Arabidopsis

**Faye M. Rosin[1,†], Naohide Watanabe[1], Jean-Luc Cacas[1], Naohiro Kato[1,‡], Juana M. Arroyo[2], Yuda Fang[2], Bruce May[2], Matthew Vaughn[2], Joseph Simorowski[2], Umamaheswari Ramu[2], Richard W. McCombie[2], David L. Spector[2], Robert A. Martienssen[2,*] and Eric Lam[1,*]**

[1]*Biotech Center, Rutgers University, 59 Dudley Rd, New Brunswick, NJ 08901, USA, and*

[2]*Cold Spring Harbor Laboratory, Cold Spring Harbor, NY 11724, USA*

Received 2 February 2008; revised 22 March 2008; accepted 26 March 2008; published online 2 June 2008.

[*]For correspondence (fax +1 732 932 6535; e-mail lam@aesop.rutgers.edu or martiens@cshl.org).

[†]Present address: Dept. of Organismic and Evolutionary Biology, Harvard University, Cambridge MA 02138, USA.

[‡]Present address: Dept. of Biological Sciences, Louisiana State University, Baton Rouge, LA 70803, USA.

**Summary**

**The interphase nucleus exists as a highly dynamic system, the physical properties of which have functional importance in gene regulation. Not only can gene expression be influenced by the local sequence context, but also by the architecture of the nucleus in three-dimensions (3D), and by the interactions between these levels via chromatin modifications. A challenging task is to resolve the complex interplay between sequence- and genome structure-based control mechanisms. Here, we created a collection of 277 Arabidopsis lines that allow the visual tracking of individual loci in living plants while comparing gene expression potential at these locations, via an identical reporter cassette. Our studies revealed regional gene silencing near a heterochromatin island, via DNA methylation, that is correlated with mobility constraint and nucleolar association. We also found an example of nucleolar association that does not correlate with gene suppression, suggesting that distinct mechanisms exist that can mediate interactions between chromatin and the nucleolus. These studies demonstrate the utility of this novel resource in unifying structural and functional studies towards a more comprehensive model of how global chromatin organization may coordinate gene expression over large scales.**

**Keywords: gene regulation, nuclear organisation, chromatin, position effects.**

The spatial organization of the interphase nucleus plays an essential role in regulating transcription (Branco and Pombo, 2007). Regional control of gene expression is based on both linear location in the genome and within the 3D nuclear space. In eukaryotes, there is significant co-expression of linearly arranged genes that do not share functional similarities (Kosak and Groudine, 2004; Ren *et al.*, 2005). For example, mapping of the human transcriptome revealed genome location-dependent clustering of highly expressed genes in regions of 5- to 15-Mbp, and similar regions of poorly expressed genes, called 'regions of increased gene expression' (ridges) and antiridges, respectively (Caron *et al.*, 2001). Interestingly, whereas the activity of individual genes may vary in a tissue-specific manner, the average transcriptional activity of the ridges and antiridges remains similar (Goetze *et al.*, 2007). Moreover, actively transcribed unlinked genes in a 40-Mbp region frequently co-localize with the same RNA polymerase II 'transcription factory' (Osborne *et al.*, 2004).

Within the nuclear space, chromosomes occupy discrete regions called chromosome territories (CTs), with chromatin further organizing into 0.2- to 2-Mbp loops (Cremer *et al.*, 2006). In Arabidopsis, transcriptionally active DNA is located in loops away from the more compact and transcriptionally silenced heterochromatic chromocenters (Fransz *et al.*, 2002). Formation of loops allows linearly distant elements

from the same or neighboring chromosomes to come into close proximity (Carter *et al.*, 2002; Lomvardas *et al.*, 2006). Conversely, genes residing near the nuclear periphery have less chance for interaction with other chromosomal regions (Lanctôt *et al.*, 2007). This lack of interaction appears to have functional relevance, as transcriptionally inactive regions were observed to localize to the nuclear periphery (Fang and Spector, 2005; Goetze *et al.*, 2007) or to the nucleolus (Zhang *et al.*, 2007). Disruption of subnuclear organization can be correlated with the release of gene silencing for some loci (Mathieu *et al.*, 2003).

Likewise, analysis of human ENCODE regions strongly supports the global organization of interphase chromosomes into distinct regions that are active or repressed in transcription (Thurman *et al.*, 2007). Examining a set of human cell lines with single insertions of a GFP reporter that was dispersed genome wide, Gierman *et al.* (2007) found a correlation between GFP reporter gene activity and the behavior of the respective domain. Thus, active GFP insertions mapped primarily to ridges, whereas repressed insertions were predominantly located in antiridges. A close examination via fluorescent *in situ* hybridization (FISH) for five lines on Chromosome 1 (Chr.1) revealed that predicted ridges are localized more centrally in the nucleus, whereas antiridges tend to localize towards the nuclear periphery. By using the same insertion construct, this study provided evidence for location-dependent changes in the likelihood, or 'potential', that transcription can be activated. However, the mechanism(s) involved in regulating this transcription potential, and the direct quantification of the predicted structural constraint on the repressed insertions, have not been addressed. Fundamentally, one can thus view that transcription is determined by at least two parameters: the *cis*-acting elements associated with the gene, and the regional environment in which the gene is located.

It has been difficult to examine regional control of gene expression in a functional and structural context at the global level. Limited collections of single-insertion Arabidopsis lines did not reveal obvious position effects, possibly because of the small numbers analyzed (De Buck *et al.*, 2004; Nagaya *et al.*, 2005; Schubert *et al.*, 2004). Moreover, structural information derived from FISH is static, and physical parameters of chromatin such as relative diffusion rate and radius cannot be extracted (Gierman *et al.*, 2007).

To overcome these difficulties, we generated a collection of Arabidopsis lines that are tagged genome wide with a single copy of a common Ds transposable element. This element is engineered to allow the quantification of gene expression in the context of nuclear structure in living plants. With 277 well-characterized lines, a genome-wide 'transcription potential' map was assembled. Detailed analysis of a 100-kbp region on Chr.2 uncovered several loci that display strong regional root-specific silencing, mediated by maintenance cytosine methylation. For one locus at least, silencing of transcriptional activity was correlated with alterations in the 3D nuclear position and chromatin dynamics.

## Results

### *Genome-wide charting of Arabidopsis chromosomes*

To chart genome position-dependent effects on gene expression, we generated a collection of Arabidopsis lines that were tagged with an identical 'chromatin charting' CCP4 gene cassette, a versatile reporter of subnuclear behavior and gene function (Figure 1a). A transposon-based strategy was utilized to minimize the frequency of complex rearrangements and duplications upon integration, as is typical for *Agrobacterium*-mediated transformation. The CCP4 cassette contains a 35S:*Luciferase* (35S:*LUC*) reporter gene to monitor relative transcription potential at the particular insertion site, an *LacO* array to allow visualization of the locus in living cells (Kato and Lam, 2003), a Nos:*NptII*:nos cassette for positive selection and a *GUS* gene with a minimal promoter (an enhancer trap) to detect enhancer activities in the neighborhood of the insertion. The constitutive 35S promoter was placed in the interior of the construct to insulate it as much as possible from enhancers or silencing elements that may be near the insertion site. As the enhancer trap and the 35S:*LUC* cassette are in the same orientation, strong enhancer activity acting in *cis* should result in the enhancement of both LUC and GUS expression. If enhancement of the 35S:*LUC* cassette is achieved through its physical location only, GUS expression will not be activated. Unlike other reporter genes, luciferase has a short half-life, thereby providing more accurate indirect quantification of transcript levels via enzyme activity measurements. These gene units are flanked by maize Ds sequences to create a functional Ds transposable element. Adjacent to the proximal Ds sequence, a 35S:*IAAH* gene conferring NAM sensitivity was added to permit negative selection for unlinked transpositions (Sundaresan *et al.*, 1995).

From 100 transgenic Arabidopsis lines (Columbia) containing the CCP4 construct, eight 'launch-pad' CCP4 lines were crossed with six CCP5 lines expressing the maize Ac-transposase and the 35S:*IAAH* counter-selection marker. Hence, the resulting transposants are not linked to the parental CCP4 locus, and the CCP5 locus is segregated away to stabilize the new insertions. Screening of 11 682 $F_2$ families by Kan/NAM selection resulted in the isolation of 611 transposition events (chromatin-charting transposants, CCT lines). The overall transposition frequency, of ~5%, is low (Sundaresan *et al.*, 1995), and this is most likely because of the large size (~12 kbp) of the Ds element in the CCP4 construct. Southern analysis revealed that only 2- to 2.4-kbp of the original 8-kbp *LacO* array was retained in the CCP4 lines. The *LacO* array is stable during transposition *in planta* because its size is maintained in the CCT lines recovered, as

 

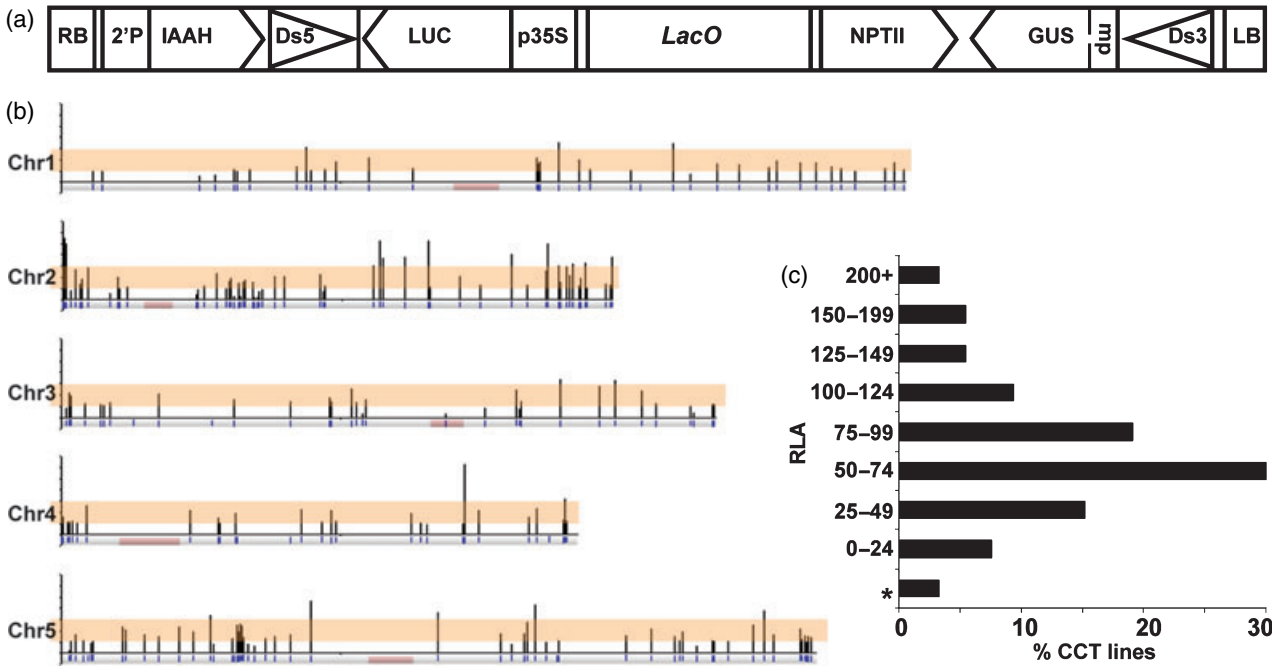


**Figure 1.** CCP4 construct and transcription potential of isolated transposants.
(a) The structure of the T-DNA used to create the CCP4 lines in Arabidopsis is shown. RB, LB, right and left borders; 2'P, promoter from T-DNA; IAAH, indole acetamide hydrolase gene; Ds, border sequences from maize Ds element; LUC, firefly luciferase; p35S, CaMV 35S promoter; *Lac*O, *lac* operator arrays; NPTII, neomycin phosphotransferase gene cassette; GUS, β-glucuronidase; mp, minimal CaMV 35S promoter (from −46 to +8 bp).
(b) The relative luciferase activity (RLA) of 2-week-old seedlings as a function of chromosomal location is shown. Chromosomes 1 (top) to 5 (bottom) are represented by a gray bar, with the centromeric region shown in red. A blue line indicates the location of individual chromatin-charting transposants (CCT) lines. The black bar above individual CCT lines represents the corresponding RLA (*y* axis), which is normalized to the activity of our control line CCP4-20 set as 100. Data represents the mean from triplicate assay samples. The region shaded in pink represents the average RLA of 50–150 relative units.
(c) Distribution of RLA in 2-week-old seedlings for our collection of 277 lines. The RLA for 80% of the CCT lines is within a twofold range, between 50–150 relative units. Asterisks denote lines with a compromised 35S:*LUC* cassette.

shown by Southern analysis (data not shown). Of the 611 transposants isolated, the location of 271 CCT and six CCP4 lines were mapped by Thermal asymmetic interlaced (TAIL)-PCR and individually confirmed by locus-specific PCR, respectively (Table S1). GUS expression was observed for 21% of these lines, thus identifying insertion sites with active enhancers (Table S2).

### *Position effects mediate transcription potential for ~20% of the collection*

Not only is transcriptional activity of a gene determined in a sequence-dependent manner by its associated *cis*-acting elements, e.g. promoters and enhancers, but it is also regulated at the chromatin and subnuclear levels. By utilizing an identical gene cassette dispersed genome wide, the effect of the regional environment on the potential for transcription activity can be compared between particular locations in the genome, with minimal interference from sequence-dependent variables. A 'transcription potential map' for all five chromosomes (Chr.) was generated by measuring relative luciferase activity (RLA) as a function of chromosomal position (Figure 1b; Table S2).

For our collection, the RLA in 80% of the CCT lines (>200 lines) is within twofold of the mean, i.e. between 50 and 150 relative units (Figure 1c). During the initial standardization of our assay for RLA, we noted that the measured activity from individual plants of homozygous, single insertion lines can vary by up to twofold. We thus set this as a significance threshold for our transcription potential map data. Thus, our resultant map indicates that for the majority of the lines insertion position does not significantly affect transgene expression. However, for 20% of the lines, there is significant silencing, of greater than 10-fold, or enhancement, of up to threefold, of RLA. For lines with very low RLA (≤11), the integrity of the 35S:*LUC* cassette was examined by PCR (data not shown). Nine CCT lines (~3% of mapped insertions) had intact 35S:*LUC* cassettes, but RLA at background levels. Additionally, three of these lines, but none of the lines with high RLA (>200), were positive for enhancer-induced GUS activity (Table S2). The latter observation is especially significant because it indicates that neighboring enhancers are unlikely to cause the heightened RLA in these lines. Our results provide clear evidence that location in the genome, not sequence-dependent effects, is likely to be responsible for the observed transcription potential differences.

*Effect of insertion location on transcription potential, subnuclear localization and diffusion dynamics*

The parental line, CCP4.211, provided further evidence that the observed differences in RLA correlate with insert location within the genome. CCP4.211 has very low RLA, and is located adjacent to the NOR and rDNA genes of Chr.2, a region populated by gypsy-like retrotransposons. The transposition efficiency of CCP4.211 was also extremely low; only nine transposants (0.7%) were isolated from the 1256 $F_2$ families produced from crosses with CCP5 lines. Whereas the RLA of CCP4.211 was highly suppressed (10-fold less than average), three of its progeny, CCT72 (Chr.2), CCT71 (Chr.3) and CCT77 (Chr.3), showed high levels of RLA (Table 1). This demonstrates that the insertion of CCP4.211 retains all elements necessary for the functional expression of the *LUC* cassette, and that regional silencing mechanisms are responsible for RLA suppression in the parental CCP4.211 locus.

In addition to significant differences in transgene activity, CCP4.211 and the progeny line CCT71 displayed differential subnuclear localization and dynamics. Visualization of the CCP4/CCT loci in living cells was accomplished by crossing with a CCV (chromatin-charting visualization) line containing an inducible fluorescent protein-Lac Repressor (LacI) fusion targeted to the nucleus (Figure S1). The LacI fusion protein is tethered to the *LacO* arrays via its DNA-binding domain, allowing the CCP4/CCT locus to be visualized as a bright spot in the diffusely fluorescing nucleoplasm. Most mature cells in the leaf are polyploid as a result of endoreduplication, and in a 16N nucleus of heterozygous plants, up to eight spots may be observed. In the CCV control line (−*LacO*) only diffuse fluorescence was observed (Figure 2a, upper panel). For CCP4.211 (located near the NOR on Chr.2), the *LacO* spots are frequently clustered around the nucleolus (Figure 2a, middle panel), whereas in CCT71 (located in the

**Table 1** Luciferase activity is recovered in progeny of CCP4.211

| Line | Chromosome | Nucleotide location | Relative luciferase activity ± SD |
|---|---|---|---|
| CCP4.211 | 2 | 10084 | 11 ± 2 |
| CCT366 | 2 | 51495 | 17 ± 3 |
| CCT383 | 2 | 94835 | 11 ± 3 |
| CCT72 | 2 | 620069 | 70 ± 11 |
| CCT399 | 2 | 1694713 | 28 ± 2 |
| CCT281 | 2 | 5547654 | 43 ± 3 |
| CCT71 | 3 | 19336732 | 141 ± 21 |
| CCT77 | 3 | 19841062 | 169 ± 37 |
| CCT76 | 3 | 22691780 | 22 ± 9 |

Transposants isolated from the mobilization of the parental line CCP4.211 are compared by chromosomal location and relative luciferase activity (RLA). Most of the progeny had higher RLA levels compared with CCP4.211.

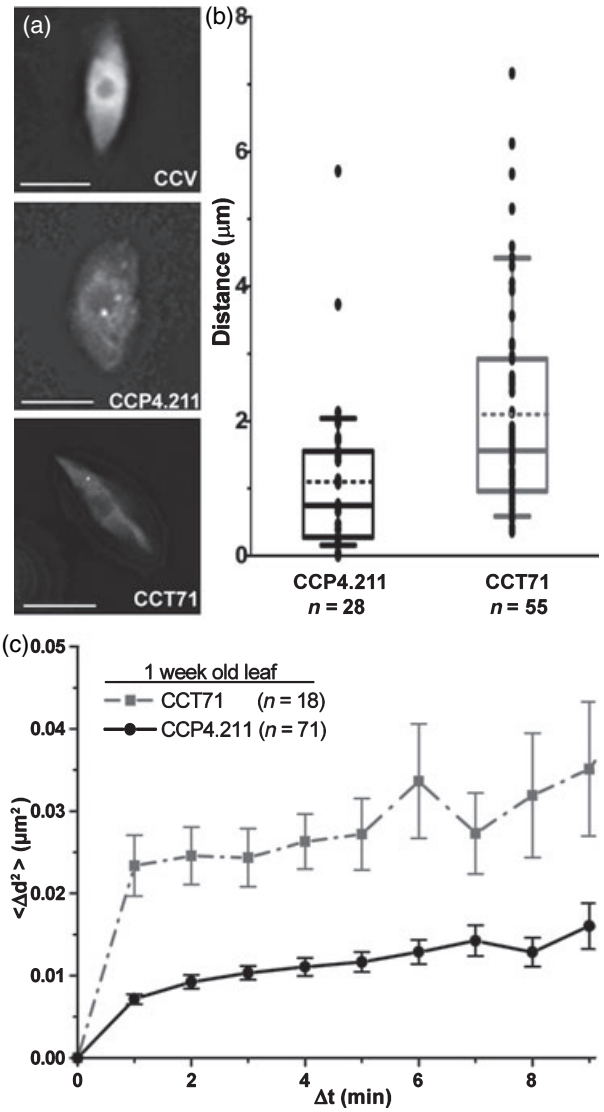


**Figure 2.** CCP4.211 is localized nearer to the nucleolus with lesser mobility than its progeny CCT71.

(a) Representative micrographs of nuclei from endoreduplicated leaf cells of 1-week-old seedlings grown on MS plates. A single *z* section is shown. The chromatin-charting visualization (CCV) control (−*LacO*, upper panel) showed diffuse fluorescent protein staining. In CCP4.211 (middle panel), spots are clustered next to the nucleolus, whereas in CCT71 (lower panel), spots are farther from the nucleolus. Scale bar: 10 μm.

(b) Box and whisker plot of the 3D distance (μm) of *LacO* spots from the edge of the nucleolus. Lower and upper whiskers are the 5th and 95th percentiles, respectively. Lower, middle and upper limits of the box represent the 25th, 50th and 75th percentiles, respectively. Dotted lines represent the mean. Filled circles represent the distance of individual spots. CCP4.211 spots are clustered next to the nucleolus. *n*: number of spots measured.

(c) The mean-squared change in 3D distances ($< \Delta d^2 >$) between two *LacO* spots over time ($\Delta t$) was plotted. Free movement is represented by a line that continuously increases over time, whereas constrained diffusion increases until it reaches a plateau. The slope represents the diffusion coefficient; the height of the plateau was used to calculate the radius of confinement. Each data point is the mean ± SE of *n* pairs of distances. CCP4.211 is highly constrained compared with CCT71.

 

middle of the short arm of Chr.3) this preference is not observed (Figure 2a, lower panel). Measuring the three-dimensional (3D) distance of the *LacO* spots from the nucleolar periphery confirms that CCP4.211 spots are preferentially localized next to the nucleolus, compared with CCT71 (Figure 2b).

To examine the effect of CCP4.211 localization near the nucleolus, submicrometer single particle tracking was used to quantify chromatin dynamics (Marshall *et al.*, 1997). By plotting the mean-squared change in 3D distances ($< \Delta d^2 >$) over time ($\Delta t$) between two *LacO* spots, the physical parameters of locus mobility can be quantified (Figure 2c). A line continuously increasing over time represents free movement. If the movement is constrained, the line will rapidly increase and then plateau. Active, directed motion would be apparent by an upward parabolic curve (Marshall *et al.*, 1997). *LacO* arrays in both CCP4.211 and CCT71 display constrained diffusion, although there is a clear difference in mobility between these two loci (Figure 2c; Table 2). The diffusion coefficient is calculated from the slope of the line ($D = \Delta d^2/4\Delta t$), and the radius of confinement is derived from the height of the plateau (Table 2). Notably, there is a strong correlation between the difference in mobility of the lines and the observed transcription potential for these two insertions. The strongly suppressed CCP4.211 displayed a confinement radius of just 0.10 μm, and is about threefold slower than CCT71, a line characterized by high transcription potential.

### *Regional effects on transcription potential*

As the dramatic suppression in transcription potential for CCP4.211 is correlated with tethering to the nucleolus and decreased mobility, we examined how other CCT lines inserted into the same region of Chr.2 behaved. There are 14 lines inserted into the first 100-kbp of the short arm of Chr.2, with RLA ranging from a low of 11 to a high of 101 relative units (Figure 3a). Additionally, specific characteristics of this region of the genome (e.g. location of genes, methylation) are shown, and were compiled from the following browsers: http://epigenomics.mcdb.ucla.edu/DNAmeth/ and http://www.arabidopsis.org/cgi-bin/gbrowse/arabidopsis/. Adjacent to the NOR and rRNA genes (light blue), there is a 50-kbp region filled with gypsy-like retrotransposons (magenta). The

**Table 2** Chromatin dynamics for different lines, tissues and treatments are shown

| Line | Tissue | Treatment | Age | Confinement radius (μm) | Diffusion coefficient ($\times 10^{-5}$ μm$^2$ sec$^{-1}$) | *P*-value |
|---|---|---|---|---|---|---|
| CCT71 | Leaf | MS | 1w | 0.16 | 9.7 | $<10^{-7}$* |
| CCP4.211 | Leaf | MS | 1w | 0.10 | 3.0 | |
| CCP4.211 | Leaf | MS | 2.5w | 0.15 | 7.4 | 0.63 |
| CCP4.211 | Leaf | AZA | 2.5w | 0.14 | 7.2 | |
| CCT431 | Leaf | MS | 2.5w | 0.14 | 6.7 | 0.45 |
| CCT431 | Leaf | AZA | 2.5w | 0.15 | 7.1 | |
| CCT396 | Leaf | MS | 2.5w | 0.15 | 6.9 | 0.45 |
| CCT396 | Leaf | AZA | 2.5w | 0.14 | 5.9 | |
| CCT432 | Leaf | MS | 2.5w | 0.12 | 4.2 | 0.009* |
| CCT432 | Leaf | AZA | 2.5w | 0.15 | 7.6 | |
| CCP4.211 | Root | MS | 2.5w | 0.14 | 7.4 | 0.028* |
| CCP4.211 | Root | AZA | 2.5w | 0.19 | 11.8 | |
| CCT71 | Root | MS | 2.5w | 0.15 | 8.6 | 0.94 |

The diffusion coefficient and radius of confinement are calculated from the graphs shown in Figures 2 and S3. A two-sample Student's *t*-test was used to test the significance of the difference between two samples at $t = 3$ min.
*Statistically significant differences, with a *P*-value < 0.05.

**Figure 3.** The short arm of chromosome 2 displays strong root-specific silencing mediated by methylation.
(a) Detail of the first 100-kbp of the short arm of chromosome 2. The gray bar represents the first 100-kbp of chromosome 2, with the location of chromatin-charting transposants (CCT) lines marked in blue. The black bar represents the corresponding relative luciferase activity (RLA) (*y* axis) for 2-week-old seedlings. Horizontal lines indicate regions and individual genes are indicated: light blue, rRNA genes; magenta, gypsy-like retrotransposons; green, genes and pseudogenes; dotted line, putative heterochromatin island. Additional information for this genomic region is also shown at http://epigenomics.mcdb.ucla.edu/DNAmeth/ and http://www.arabidopsis.org/cgi-bin/gbrowse/arabidopsis/, including prevalence and location of expressed sequence tags (ESTs), T-DNAs/transposons, smallRNAs and %GC content. Cytosine methylation in aerial plant tissues is shown for wild type, the *met1* single mutant and the *dcc* triple mutant in the Col-0 background.
(b) Detection of tissue-specific position effects on RLA. RLA was measured for either leaf or root tissues of 2.5-week-old seedlings. Asterisks denote lines with root-specific silencing.
(c) Reversal of silencing in root tissues by treatment with DNA methylation inhibitor 5-aza-2′-deoxycytidine (AZA). Asterisks denote lines with increased RLA after AZA treatment.
RLA was calculated by setting the observed activity from seedlings (a) or shoot tissue (b and c) of our reference line, CCP4-20, to 100. Data represents the mean ± SE.

 

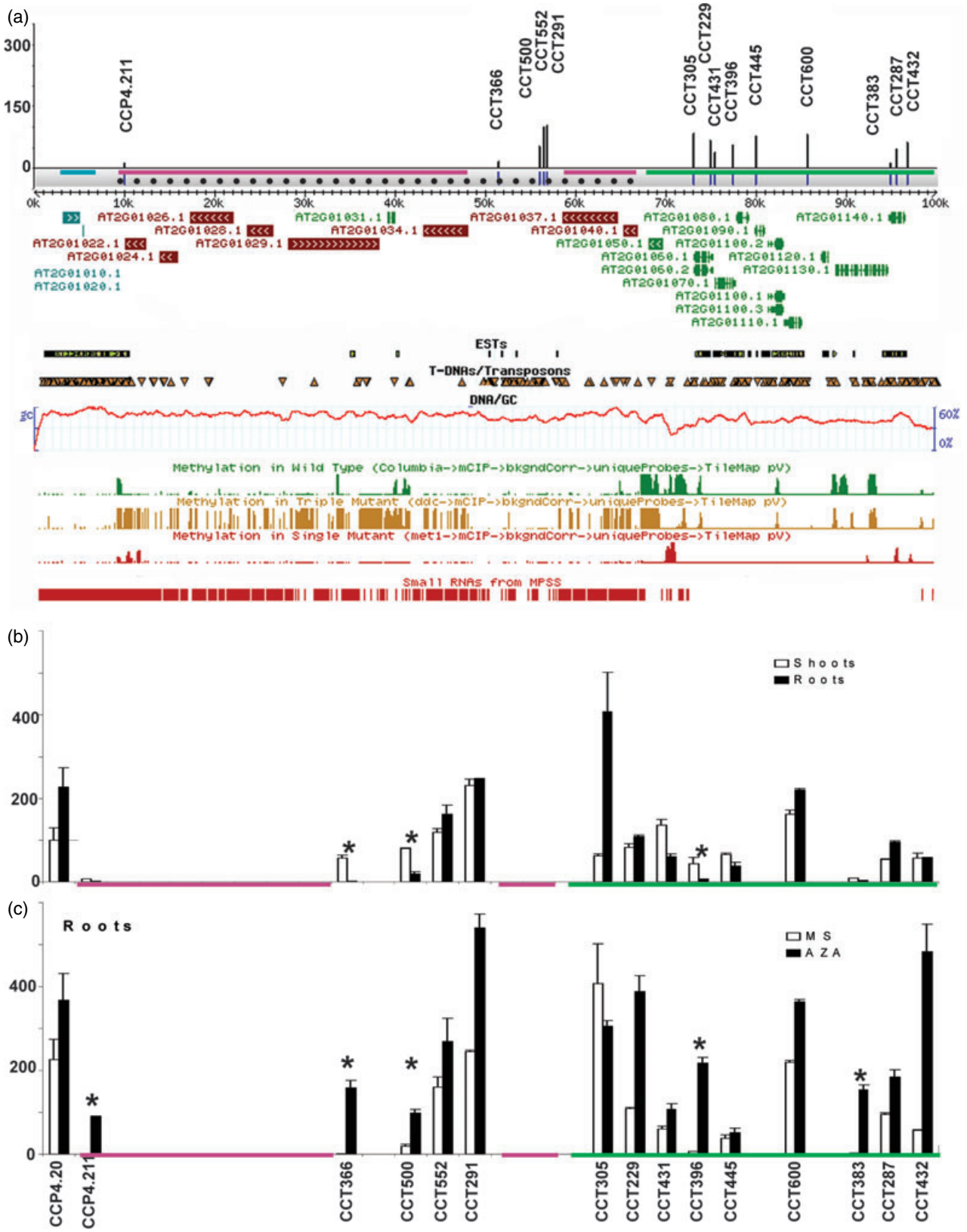


 

lack of gene transcript representation in expressed sequence tag (EST) libraries and the high prevalence of small RNAs detected by massively parallel sequencing (MPSS) suggest that this region is heterochromatized (dotted line). Although we did not recover any transposants inserted into a gypsy-like retrotransposon, there is a small window of about 9-kbp between retrotransposon-like sequences where four insertion lines were recovered. Three of the lines have average activities in seedlings, whereas CCT366 is highly suppressed. Most CCT lines inserted into or near putative genes (green) display close-to-average activities, with the exception of CCT383. These results suggest that insertion near retrotransposons can significantly affect transcription potential.

Furthermore, we detected strong root-specific suppression in several lines (Figure 3b, asterisks), mainly around the heterochromatin island. We found that this root-specific suppression was likely to be mediated by DNA methylation. The lines in this region were treated on MS plates ± a DNA methylation inhibitor, 5-aza-2′-deoxycytidine (AZA) or MS, respectively (Chang and Pikaard, 2005). There was a clear induction of activity in the roots from lines displaying strong suppression (Figure 3c, asterisks). Conversely, there was little difference in shoot RLA after AZA treatment (Figure S2). This suggests that there is regional epigenetic control of transcription potential under different developmental contexts. The root-specific and reversible nature of transcriptional silencing in loci such as CCT366, CCT396 and CCT383 demonstrates that these insertions are structurally intact, and that their low RLA is the result of epigenetic control. Consistent with this interpretation, preliminary experiments to access methylation of the inserts using McrBC-PCR assays indicated that there was differential cytosine methylation amongst the CCT lines (FR, unpublished data). The *LacO* repeats and the 35S promoter, but not the *LUC* gene, are apparently methylated to varying degrees in these lines. Although we have not examined the flanking genomic sequences in our assays, available data for cytosine methylation in wild type (Figure 3a, green panel) indicates that there is methylation flanking some (e.g. CCP4.211 and CCT383), but not all (e.g. CCT366 and CCT500), of the CCT lines displaying AZA-induced LUC expression.

### *CCP4.211 activity is restored earlier in* met1-1 *compared with* ddm1-2 *mutants*

In parallel with the chemical approach, a genetic approach was undertaken by crossing CCP4.211 into two different methylation mutant backgrounds (Vongs *et al.*, 1993). *MET1* is a CpG methyltransferase and *DDM1* (decreased DNA methylation 1) is a SWI2/SNF2-like chromatin remodeler (Jeddeloh *et al.*, 1999; Kankel *et al.*, 2003). Both genes are involved in maintenance DNA methylation, and mutants display genome-wide hypomethylation (Lippman *et al.*, 2004; Zhang *et al.*, 2006a). In the heterozygous mutant $F_1$ generation, there was no change in CCP4.211 RLA, as expected (Figure 4a). Notably, the presence of only one copy of the CCP4 transgene does not relieve silencing. This emphasizes that allelic pairing between the inserted repeat arrays, if present in the homozygous state, is not necessary to maintain silencing in this locus. In the $F_2$ homozygous *met1-1* background, the CCP4.211 activity was restored to normal levels: a ~10-fold increase (Figure 4b). *ddm1-2* did not rescue the activity of CCP4.211 in the $F_2$ generation; however, in the $F_3$ and $F_4$ generations, the activity of CCP4.211 increased markedly to above 300 relative units (Figure 4c). Together with our data for AZA treatments, these genetic data show that cytosine methylation has a dramatic effect on relieving transgene silencing for several lines inserted in this region of Chr.2.

### *Regional effects on subnuclear organization and dynamics*

To compare regional effects on subnuclear organization and dynamics in response to AZA, we selected four lines in this region for visualization in living cells. CCP4.211 was shown to be closely associated with the nucleolus and to have limited mobility, along with highly suppressed activity. CCT431 and CCT396 are inserted close to each other but respond differently to AZA treatment. CCT432 is located at the end of the 100-kbp region with average RLA. Figures 5(a,b) are maximum-intensity projections of 40 *z* sections for leaf or root nuclei, respectively, from 2.5-week-old seedlings with MS (upper panels) or AZA (lower panels) treatment. Our CCV lines show strong silencing in a tissue-specific manner, making it difficult to visualize root tissues. Furthermore, it was difficult to distinguish the nucleolus clearly in CCP4.211 MS roots and CCT431 AZA leaves. Only diffuse nuclear staining is observed in the control CCV line. In CCP4.211 MS leaves and roots, multiple spots are clustered around the nucleolus, whereas upon AZA treatment, some *LacO* spots moved away from the nucleolus. Measurement of the distance of *LacO* spots from the nucleolar periphery (Figure 5c) revealed that AZA exerted a significantly greater influence on CCP4.211 roots compared with leaves ($P = 0.004$). For CCT431 and CCT396, there is no apparent preferential localization of *LacO* spots (Figure 5a); however, distance measurements (Figure 5c) indicated that CCT396 AZA spots, compared with MS spots, are more closely tied to the nucleolus ($P = 0.03$). Unexpectedly, the CCT432 locus exhibits a pronounced preference for the nucleolar periphery in both MS and AZA leaves, similar to CCP4.211 MS (Figure 5a,c).

Chromatin dynamics and response to epigenetic modification varied with tissue (Table 2; Figure S3). Similar to changes in RLA and spot localization, AZA had a more significant effect on mobility in CCP4.211 roots compared with leaves. The confinement radius and diffusion coefficient significantly increased in CCP4.211 AZA roots compared with

 

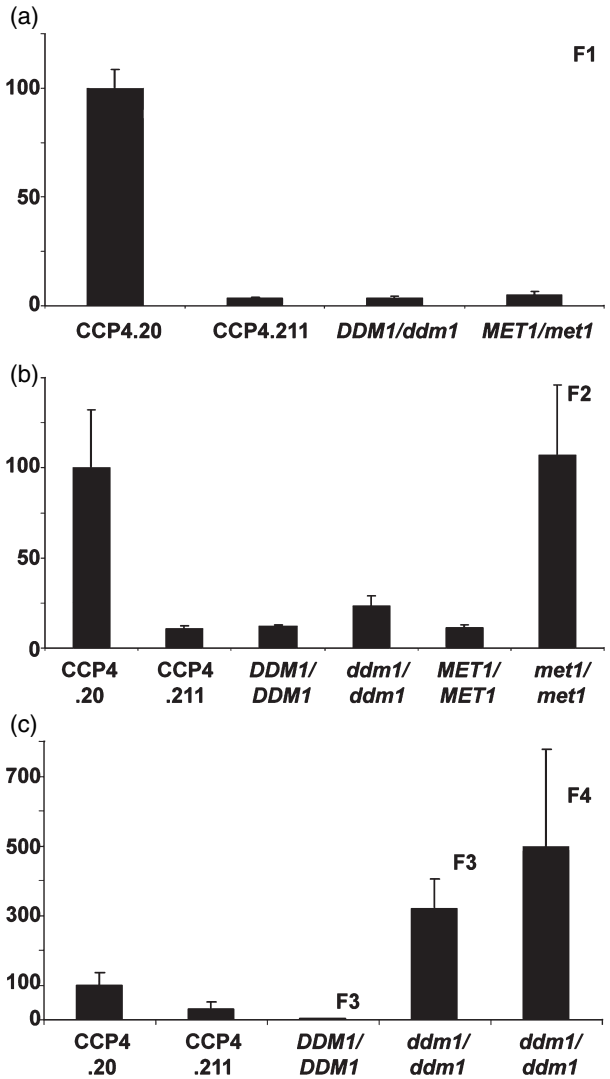


**Figure 4.** Relative luciferase activity (RLA) for CCP4.211 is recovered in both the homozygous *met1-1* and *ddm1-2* backgrounds.
RLA was measured *in vivo* for one leaf per seedling, and the mean ± SE is shown. RLA was calculated by setting the reference line CCP4.20 to 100.
(a) CCP4.211 RLA remains suppressed in the heterozygous $F_1$ generation.
(b) RLA for CCP4.211 in the $F_2$ generation is shown. CCP4.211 exhibited a small twofold increase in RLA in the *ddm1-2* homozygous background. In the *met1-1* homozygous background, CCP4.211 RLA was restored to control levels: a 10-fold increase.
(c) CCP4.211 RLA is shown for the $F_3$ and $F_4$ generations in the homozygous *ddm1-2* background. CCP4.211 activity was recovered to very high levels, above 300 relative units.

MS roots or MS and AZA leaves (Table 2). Leaves had approximately the same radius of confinement and diffusion coefficient as MS roots, regardless of treatment with AZA. Spot mobility was similar in CCT431 and CCT396 with regards to confinement radii and diffusion coefficients, for both MS and AZA leaves (Table 2). CCT432, however, displayed a significant increase in mobility for AZA compared with MS leaves, without an accompanying change in RLA (Table 2).

## Discussion

A transcription potential map was generated for 2-week-old Arabidopsis seedlings utilizing a collection of 277 transgenic lines containing an identical gene cassette. Whereas approximately 80% of the lines had similar levels of reporter gene transcription, the remaining 20% displayed elevated or silenced transcriptional activity (Figure 1), suggesting position effects. Although previous reports did not detect clear evidence for position effects on transgene expression, this was likely to be because of the limited number of lines examined (<30) with the same reporter gene and in the same vector context (De Buck *et al.*, 2004; Nagaya *et al.*, 2005; Schubert *et al.*, 2004). This makes straightforward comparisons of transcriptional activity based on location ambiguous.

About 80% of our collection, over 200 lines, exhibited similar RLA levels, suggesting that the number of lines examined in previous reports was probably too small to identify genomic loci with position effects. The parental line, CCP4.211, provided further evidence that the observed differences in activity correlate with insert location within the genome. Mobilization of the inserted element in this highly suppressed line resulted in recovery of higher levels of RLA in most of the resultant transposants (Table 1). In addition to recovered RLA, CCT71 exhibited differential nuclear localization and less constrained mobility compared with its parent CCP4.211 (Figure 2). This indicates that transcription activity is correlated with chromatin dynamics and location in the genome for this locus.

### *DNA methylation mediates transcription suppression in the first 100-kbp of Chr.2*

Using both genetic and chemical approaches to reduce DNA methylation, RLA for CCP4.211 was increased to levels seen in non-silenced insertion lines. Interestingly, there was a differential effect of hypomethylation in two different mutant backgrounds (Figure 4). In the $F_2$ generation, the *met1-1* homozygous background resulted in RLA recovery in leaves of CCP4.211 plants, whereas the *ddm1-2* background had little effect. Succeeding generations in the homozygous *ddm1-2* background resulted in a striking increase of CCP4.211 RLA to over 300 relative units. This difference suggests that the role of DDM1 in gene silencing at this locus may be more indirect or complex. Recent observations that DDM1 may function to define heterochromatin boundaries also suggest that its mode of action may be complex (Saze and Kakutani, 2007).

For several other lines inserted in the same region of Chr.2, AZA treatment revealed strong root-specific silencing mediated by methylation (Figure 3). Conversely, blocking histone deacetylation by trichostatin A treatment did not affect RLA in this region (data not shown). This suggests that

 

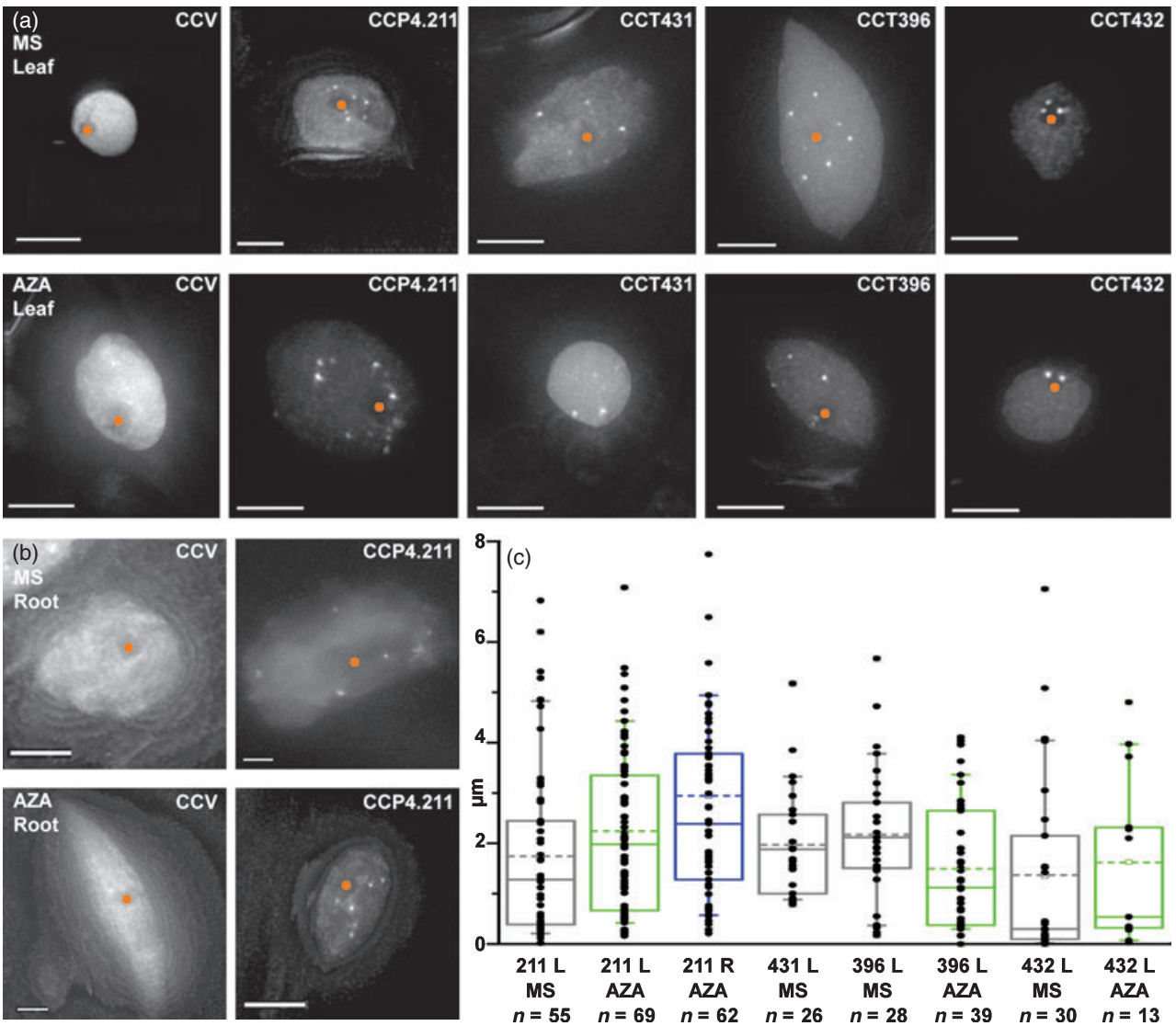


**Figure 5.** Localization of chromatin-charting transposants (CCT) loci from the short arm of chromosome 2.
Micrographs and measurements are from endoreduplicated leaf or root nuclei from 2.5-week-old seedlings. Micrographs are maximum-intensity projections of 40 *z* sections; scale bar = 5 μm. The nucleolus generally shows lighter diffused florescence than the surrounding nucleoplasmic space. Its center is marked with a red dot.
(a) Representative micrographs for MS (upper panels) or 5-aza-2′-deoxycytidine (AZA) treatment (lower panels) in leaf pavement cells. Chromatin-charting visualization (CCV) control lines (–*LacO*) display diffuse staining throughout the nucleus, but do not display spots. CCP4.211 spots are tightly clustered next to the nucleolus; however, after treatment with AZA, CCP4.211 spots are further away from the nucleolus. In MS and AZA seedlings, spot localization is similar for CCT431, CCT396 and CCT432.
(b) Representative micrographs of root nuclei for MS (upper panels) and AZA (lower panels) treatment for CCV control lines (left) and CCP4.211 (right). In the AZA root nuclei of CCP4.211, *LacO* spots no longer cluster next to the nucleolus.
(c) Box and whisker plot of 3D distance of *LacO* spots from the periphery of the nucleolus for each line. Boxes are gray for MS leaves, green for AZA leaves and blue for AZA roots. Black circles represent the distance for individual spots. CCP4.211 AZA roots are significantly farther away from the nucleolar periphery than CCP4.211 MS or AZA leaves. CCT432 spots are confined to the nucleolus. *n*: number of spots measured.

DNA methylation, rather than histone deacetylation, is the predominant epigenetic regulator of silencing in this region. This is in contrast to previous studies that showed suppression of histone deacetylation, by trichostatin A or RNA silencing strategies, reactivated rDNA transcription in the epigenetic phenomenon known as nucleolar dominance (Chang and Pikaard, 2005; Chen and Pikaard, 1997). Our results thus show that gene silencing at or near the NOR on Chr.2 is distinct from that observed for nucleolar dominance, although DNA methylation appears to be involved in both cases.

A strong root-specific silencing was observed for several lines located in this 100-kbp region of Chr.2. This silencing is mediated by methylation, as inferred by the recovery of RLA after AZA treatment. We did not observe similar differences between roots and shoots for additional CCT lines located

outside this region (data not shown). This suggests that there is regional epigenetic control of transcription potential under different developmental contexts. Similar cell-type specific changes in local chromatin structure have been inferred at the *GL2* locus during root hair cell fate determination in Arabidopsis (Costa and Shaw, 2006).

### *Position in nucleus does not always correlate with transcription potential*

Our results support the existence of multiple silencing mechanisms as subnuclear position does not always correlate with transcription activity. Localization to the nuclear periphery or the nucleolus has been found to be a potent mediator of silencing (Wang *et al.*, 2005; Zhang *et al.*, 2007). In human cells, disruption of the nucleolus, and the subsequent loss of nucleolar localization for specific loci, resulted in an increase in the confinement radius that was reversed upon nucleolus reformation (Chubb *et al.*, 2002). This agrees with our findings in which CCP4.211 nucleolus localization correlates with low transcription activity. In roots, changes in subnuclear localization by hypomethylation released silencing and resulted in increased movement, with a larger confinement radius and a higher diffusion coefficient. This indicates that the heterochromatin island at the short arm of Chr.2 (Figure 3a) mediates the silencing of gene expression through tighter association with the nucleolus. Genetic and chemical studies revealed that this is likely to require CpG maintenance methylation.

CCT432 *LacO* spots (Figure 5) are also frequently linked to the nucleolus, but silencing is not observed. Treatment with AZA significantly increased the mobility of the locus without altering its subnuclear localization or associated luciferase expression in leaves. Thus, although maintenance methylation is again associated with changes in mobility, nucleolar association per se is not sufficient for transcriptional silencing. Additional experiments using more lines and genetic analyses examining epigenetic regulators that are independent of DNA methylation (e.g. *Mom1*; Amedeo *et al.*, 2000) may help resolve this complexity.

A collection of lines with an identical reporter gene allowed the quantification of transcription potential throughout the Arabidopsis genome. Significant position effects were observed in ~20% of the collection. We discovered regional control of transcriptional activity in root-specific silencing, mediated by DNA methylation. Epigenetic control of subnuclear localization and chromatin dynamics was also observed for loci in this region. These studies illustrate that this collection of transgenic lines are a valuable resource with a broad range of applications, including the discovery of tissue-specific epigenetic regulatory mechanisms. In addition, physical changes in chromatin behavior at the locus of interest can be monitored in living cells. This is in contrast to the more limited applications of GFP-tagged cell lines used in the recent work of Gierman *et al.* (2007). With a densely tagged region at the short arm of Chr.2, our results also revealed that small domains (microloops) of 2- to 3-kbp can exist as euchromatin within large heterochromatic regions (e.g. CCT552 and CCT291), although the converse may also occur (e.g. CCT383). Thus, the structure of the genome in the interphase nucleus may be more heterogeneous than previous models suggested. Proximity to islands of transposable elements seems to be an important factor in silencing, as is the case in *Drosophila* (Haynes *et al.*, 2006; Sun *et al.*, 2004). In addition to regions showing gene silencing, our collection also identified at least seven genomic loci that show significant enhancement of transcription potential, which apparently do not involve neighboring *cis*-acting enhancer elements, as the GUS enhancer trap is not activated in these lines. Study of these insertions may shed light on positive epigenetic factors in plants. By coupling quantitative transcriptional activity with an *in vivo* visualization tagging system for defined insertions throughout the genome, the chromatin-charting lines provide a powerful tool to examine chromatin-based mechanisms of gene regulation in different tissues and cell types during development.

## Experimental procedures

### *Isolation and screening of CCT lines*

Construction of the pCCP4 vector is described in Appendix S1. The binary vector pAJ1 (AY218787) was used to generate the CCP5 lines. pCCP4 and pAJ1 were transformed into *Agrobacterium tumefaciens* (strain GV3103/MP90) for transformation of Arabidopsis, Columbia ecotype, using the floral-dip method (Zhang *et al.*, 2006b). Over 100 primary transformants were selected by $Kan^R$ and were characterized by Southern blotting to determine T-DNA copy number (data not shown). Homozygous lines were isolated by segregation of $Kan^R$. For mobilization of the Ds element, eight CCP4 and six CCP5 lines were crossed in all possible combinations. $F_1$ lines were allowed to self, and $F_2$ seedlings that were $Kan^RNAM^R$ were transferred to soil (Sundaresan *et al.*, 1995). Inflorescences were collected for genomic DNA extraction (DNeasy 96 Plant Kit; Qiagen, http://www.qiagen.com) and TAIL-PCR mapping (Liu *et al.*, 1995). Seeds were harvested and stored as the $F_3$ generation transposant CCT line. The $F_3$ generation for CCT lines and at least the $F_5$ generation for CCP4 lines were used for all luciferase assays and crosses with CCV lines (with the next generation used for microscopy).

### *Treatment with AZA*

Sterilized seeds were sown on MS (0.5× MS, 1% sucrose, 0.25% phytagel) supplemented with Kanamycin (50 mg $l^{-1}$), except CCP4.211, which was germinated without antibiotic. After sowing, plates were incubated for 2 days at 4°C and were then transferred to a growth chamber with continuous light at 22°C. Then, 1.5 week-old seedlings were transferred onto fresh MS plates supplemented with 0 (MS) or 7 μg $ml^{-1}$ AZA (A3656; Sigma-Aldrich, http://www.sigmaaldrich.com) (Chang and Pikaard, 2005). Luciferase assays

 

and microscopy were performed 7 days and 4–8 days post-transfer, respectively.

### *Luciferase assays*

Luciferase activity was determined using the Promega Luciferase Assay Kit (Promega, http://www.promega.com) according to the manufacturer's instructions. The luminescence was measured using a micro-titer plate reader (Synergy HT, Multidetection; BioTek, http://www.biotek.com). Each kinetic point was performed in triplicate. The enzymatic activity was normalized with the protein concentration, determined by the Bradford method. Relative activity was normalized to the reference line CCP4.20 set as 100. The reference line is included in every experiment in order to compare data from different experiments.

### *Methylation mutants*

Homozygous CCP4.211 was crossed into homozygous *met1-1* or *ddm1-2* mutants. The $F_1$ generation was selfed, and lines homozygous for the mutation were selected by PCR and restriction fragment length polymorphisms, as described previously (Kankel *et al.*, 2003). RLA was measured *in vivo*. One leaf per seedling was weighed and placed abaxial side up in a 96-well plate containing MS media, and was sprayed with 1 mM D-Luciferin (Biogold, http://www.goldbio.com) and 0.01% Triton X-100. Luminescence was measured as described above, and was normalized by leaf weight. Relative activity was normalized to the reference line, CCP4.20. The mean ± SE of between four and seven homozygous lines each is shown.

### *Microscopy and data analysis*

A DeltaVision restoration microscope system (Applied Precision, http://www.appliedprecision.com) with either an IX71 microscope, equipped with an UPLANAPO water immersion objective lens (60×, numerical aperture 1.20; Olympus, http://www.olympus-global.com) and a CoolSNAP HQ camera (Photometrics, http://www.photomet.com), or a TE200 microscope, equipped with a PlanApo water immersion objective lens (60×, numerical aperture 1.20; Nikon, http://www.nikon.com) and a CH350 camera (Photometrics), and the appropriate filters were used for fluorescence restoration microscopy. Homozygous CCP4 or CCT lines were crossed with a CCV line: JM71 or EL700S (Figure S1). $F_1$ seedlings hemizygous for the CCP4 or CCT locus were used. FP-LacI-NLS fusion protein was induced on MS plates with 1% ethanol vapor overnight (JM71), or 0.3 μM dexamethasone (Sigma-Aldrich) for 2 days (EL700S). A single 40-frame, 0.2-μm step, *z*-stack was collected every minute for 10 min. Representative micrographs (single *z* frame) or maximum intensity projections (40 *z* frames) are shown. Not all spots are always visible because of different background levels in different *z* sections. SoftWoRx software (Applied Precision, http://www.appliedprecision.com) was used for deconvolution and subsequent measurements. Statistically significant *LacO* spots were determined as described previously (Kato and Lam, 2003). The brightest pixel of the spot was defined as its precise position, and was used for subsequent measurements. The distance of the *LacO* spot to the nucleolar periphery was determined as follows: the center of the nucleolus was first fixed so that it was the same for each of the *LacO* spots in the nucleus. The distance from this fixed center to the *LacO* spot was measured in 3D. Then, following the trajectory line generated by the software, we measured the distance from the fixed center to the nucleolar periphery, also in 3D. The final distance (shown in Figures 2b and 5c) resulted from subtraction of the two values. The mean-squared change in distances relative to $t = 0$ ($< \Delta d^2 >$) are calculated as described by Kato and Lam (2003). Calculating the change in distances between two spots, rather than calculating the changes in position of a single spot, is necessary to compensate for nuclear rotation, which may result in apparent motion.

### *Statistical analysis*

Statistical relevance was analyzed with the two-sample Student's *t*-test to test the null hypothesis that two data sets show the same distribution. A *P*-value < 0.05 was considered statistically significant. All data points for each comparison were used to determine the difference in localization. For dynamic data, values at $t = 3$ min were used for each comparison.

## Acknowledgements

We thank C.-Y. Luo for lively discussions and assistance, and D. Hannapel for critically reading the manuscript. The sharing of the JM71 vector from Josh Mlyne and Caroline Dean before its publication is gratefully acknowledged. This work is supported by a grant from the NSF Plant Genome Research Program (DBI-0077617). The authors declare no competing interests.

## Supplementary Material

The following supplementary material for this article is available online:

**Figure S1.** The structure of the T-DNAs used to create the chromatin-charting visualization (CCV) lines in Arabidopsis is shown.

**Figure S2.** Relative luciferase activity (RLA) in shoots after treatment with 5-aza-2′-deoxycytidine (AZA).

**Figure S3.** Chromatin dynamics are altered for roots, but not leaves, treated with 5-aza-2′-deoxycytidine (AZA).

**Table S1.** Primers used for locus-specific PCR and ABRC stock numbers are listed for the CCP4, CCP5 and CCT lines.

**Table S2.** Chromosomal position, relative luciferase activity (RLA) and overall level of GUS activity is given for each line in the collection.

**Appendix S1.** Protocol: more details of the construction of the CCP4 cassette.

This material is available as part of the online article from http://www.blackwell-synergy.com.

Please note: Blackwell publishing are not responsible for the content or functionality of any supplementary materials supplied by the authors. Any queries (other than missing material) should be directed to the corresponding author for the article.

## References

**Amedeo, P., Habu, Y., Afsar, K., Scheid, O.M. and Paszkowski, J.** (2000) Disruption of the plant gene MOM releases transcriptional silencing of methylated genes. *Nature*, **405**, 203–206.

**Branco, M.R. and Pombo, A.** (2007) Chromosome organization: new facts, new models. *Trends Cell Biol.* **17**, 127–134.

**Caron, H., Schaik, B.v., Mee, M.v.d. *et al.*** (2001) The human transcriptome map: clustering of highly expressed genes in chromosomal domains. *Science*, **291**, 1289–1292.

 

**Carter, D., Chakalova, L., Osborne, C.S., Dai, Y.-f. and Fraser, P.** (2002) Long-range chromatin regulatory interactions in vivo. *Nat. Genet.* **32**, 623–626.

**Chang, S. and Pikaard, C.S.** (2005) Transcript profiling in Arabidopsis reveals complex responses to global inhibition of DNA methylation and histone deacetylation. *J. Biol. Chem.* **280**, 796–804.

**Chen, Z.J. and Pikaard, C.S.** (1997) Epigenetic silencing of RNA polymerase I transcription: a role for DNA methylation and histone modification in nucleolar dominance. *Genes Dev.* **11**, 2124–2136.

**Chubb, J.R., Boyle, S., Perry, P. and Bickmore, W.A.** (2002) Chromatin motion is constrained by association with nuclear compartments in human cells. *Curr. Biol.* **12**, 439–445.

**Costa, S. and Shaw, P.** (2006) Chromatin organization and cell fate switch respond to positional information in Arabidopsis. *Nature*, **439**, 493–496.

**Cremer, T., Cremer, M., Dietzel, S., Muller, S., Solovei, I. and Fakan, S.** (2006) Chromosome territories – a functional nuclear landscape. *Curr. Opin. Cell Biol.* **18**, 307–316.

**De Buck, S., Windels, P., De Loose, M. and Depicker, A.** (2004) Single-copy T-DNAs integrated at different positions in the Arabidopsis genome display uniform and comparable β-glucuronidase accumulation levels. *CMLS Cell. Mol. Life Sci.* **61**, 2632–2645.

**Fang, Y. and Spector, D.L.** (2005) Centromere positioning and dynamics in living Arabidopsis plants. *Mol. Biol. Cell*, **16**, 5710–5718.

**Fransz, P., de Jong, J.H., Lysak, M., Castiglione, M.R. and Schubert, I.** (2002) Interphase chromosomes in Arabidopsis are organized as well defined chromocenters from which euchromatin loops emanate. *Proc. Natl Acad. Sci. USA*, **99**, 14584–14589.

**Gierman, H.J., Indemans, M.H.G., Koster, J., Goetze, S., Seppen, J., Geerts, D., van Driel, R. and Versteeg, R.** (2007) Domain-wide regulation of gene expression in the human genome. *Genome Res.* **17**, 1286–1295.

**Goetze, S., Mateos-Langerak, J., Gierman, H.J., de Leeuw, W., Giromus, O., Indemans, M.H.G., Koster, J., Ondrej, V., Versteeg, R. and van Driel, R.** (2007) The three-dimensional structure of human interphase chromosomes is related to the transcriptome map. *Mol. Cell. Biol.* **27**, 4475–4487.

**Haynes, K.A., Caudy, A.A., Collins, L. and Elgin, S.C.R.** (2006) Element 1360 and RNAi components contribute to HP1-dependent silencing of a pericentric reporter. *Curr. Biol.* **16**, 2222–2227.

**Jeddeloh, J.A., Stokes, T.L. and Richards, E.J.** (1999) Maintenance of genomic methylation requires a SWI2/SNF2-like protein. *Nat. Genet.* **22**, 94–97.

**Kankel, M.W., Ramsey, D.E., Stokes, T.L., Flowers, S.K., Haag, J.R., Jeddeloh, J.A., Riddle, N.C., Verbsky, M.L. and Richards, E.J.** (2003) Arabidopsis MET1 cytosine methyltransferase mutants. *Genetics*, **163**, 1109–1122.

**Kato, N. and Lam, E.** (2003) Chromatin of endoreduplicated pavement cells has greater range of movement than that of diploid guard cells in *Arabidopsis thaliana*. *J. Cell Sci.* **116**, 2195–2201.

**Kosak, S.T. and Groudine, M.** (2004) Form follows function: the genomic organization of cellular differentiation. *Genes Dev.* **18**, 1371–1384.

**Lanctôt, C., Cheutin, T., Cremer, M., Cavalli, G. and Cremer, T.** (2007) Dynamic genome architecture in the nuclear space: regulation of gene expression in three dimensions. *Nat. Rev. Genet.* **8**, 104–115.

**Lippman, Z., Gendrel, A.-V., Black, M. *et al.*** (2004) Role of transposable elements in heterochromatin and epigenetic control. *Nature*, **430**, 471–476.

**Liu, Y.G., Mitsukawa, N., Oosumi, T. and Whittier, R.F.** (1995) Efficient isolation and mapping of *Arabidopsis thaliana* T-DNA insert junctions by thermal asymmetic interlaced PCR. *Plant J.* **8**, 457–463.

**Lomvardas, S., Barnea, G., Pisapia, D.J., Mendelsohn, M., Kirkland, J. and Axel, R.** (2006) Interchromosomal interactions and olfactory receptor choice. *Cell*, **126**, 403–413.

**Marshall, W.F., Straight, A., Marko, J.F., Swedlow, J., Dernburg, A., Belmont, A., Murray, A.W., Agard, D.A. and Sedat, J.W.** (1997) Interphase chromosomes undergo constrained diffusional motion in living cells. *Curr. Biol.* **7**, 930–939.

**Mathieu, O., Jasencakova, Z., Vaillant, I., Gendrel, A.-V., Colot, V., Schubert, I. and Tourmente, S.** (2003) Changes in 5S rDNA chromatin organization and transcription during heterochromatin establishment in Arabidopsis. *Plant Cell*, **15**, 2929–2939.

**Nagaya, S., Kato, K., Ninomiya, Y., Horie, R., Sekine, M., Yoshida, K. and Shinmyo, A.** (2005) Expression of randomly integrated single complete copy transgenes does not vary in *Arabidopsis thaliana*. *Plant Cell Physiol.* **46**, 438–444.

**Osborne, C.S., Chakalova, L., Brown, K.E. *et al.*** (2004) Active genes dynamically colocalize to shared sites of ongoing transcription. *Nat. Genet.* **36**, 1065–1071.

**Ren, X.-Y., Fiers, M.W.E.J., Stiekema, W.J. and Nap, J.-P.** (2005) Local coexpression domains of two to four genes in the genome of Arabidopsis. *Plant Physiol.* **138**, 923–934.

**Saze, H. and Kakutani, T.** (2007) Heritable epigenetic mutation of a transposon-flanked Arabidopsis gene due to lack of the chromatin-remodeling factor DDM1. *EMBO J.* **26**, 3641–3652.

**Schubert, D., Lechtenberg, B., Forsbach, A., Gils, M., Bahadur, S. and Schmidt, R.** (2004) Silencing in Arabidopsis T-DNA transformants: the predominant role of a gene-specific RNA sensing mechanism versus position effects. *Plant Cell*, **16**, 2561–2572.

**Sun, F.-L., Haynes, K., Simpson, C.L., Lee, S.D., Collins, L., Wuller, J., Eissenberg, J.C. and Elgin, S.C.R.** (2004) *cis*-acting determinants of heterochromatin formation on *Drosophila melanogaster* chromosome four. *Mol. Cell. Biol.* **24**, 8210–8220.

**Sundaresan, V., Springer, P., Volpe, T., Haward, S., Jones, J.D., Dean, C., Ma, H. and Martienssen, R.** (1995) Patterns of gene action in plant development revealed by enhancer trap and gene trap transposable elements. *Genes Dev.* **9**, 1797–1810.

**Thurman, R.E., Day, N., Noble, W.S. and Stamatoyannopoulos, J.A.** (2007) Identification of higher-order functional domains in the human ENCODE regions. *Genome Res.* **17**, 917–927.

**Vongs, A., Kakutani, T., Martienssen, R.A. and Richards, E.J.** (1993) *Arabidopsis thaliana* DNA methylation mutants. *Science*, **260**, 1926–1928.

**Wang, L., Haeusler, R.A., Good, P.D., Thompson, M., Nagar, S. and Engelke, D.R.** (2005) Silencing near tRNA genes requires nucleolar localization. *J. Biol. Chem.* **280**, 8637–8639.

**Zhang, X., Henriques, R., Lin, S.-S., Niu, Q.-W. and Chua, N.-H.** (2006a) *Agrobacterium*-mediated transformation of *Arabidopsis thaliana* using the floral dip method. *Nat. Protocols*, **1**, 641–646.

**Zhang, X., Yazaki, J., Sundaresan, A. *et al.*** (2006b) Genome-wide high-resolution mapping and functional analysis of DNA methylation in Arabidopsis. *Cell*, **126**, 1189–1201.

**Zhang, L.-F., Huynh, K.D. and Lee, J.T.** (2007) Perinucleolar targeting of the inactive X during S phase: evidence for a role in the maintenance of silencing. *Cell*, **129**, 693–706.

 